FEBS Letters 583 (2009) 1090–1095

FEBS Letters

journal homepage: www.FEBSLetters.org

Association of the eukaryotic V_1V_O ATPase subunits *a* with *d* and *d* with A

Youg R. Thaker [1], Cornelia Hunke [1], Yin H. Yau, Susana Geifman Shochat, Ying Li, Gerhard Grüber *

School of Biological Sciences, Nanyang Technological University, 60 Nanyang Drive, Singapore 637551, Republic of Singapore

ARTICLE INFO

Article history:
Received 23 January 2009
Revised 4 March 2009
Accepted 5 March 2009
Available online 14 March 2009

Edited by Peter Brzezinski

Keywords:
Vacuolar-type ATPase
V_1V_O ATPase
Subunit *a*
Subunit *d*
Subunit A
Surface plasmon resonance
NBD-Cl

ABSTRACT

Owing to the complex nature of V_1V_O ATPases, identification of neighboring subunits is essential for mechanistic understanding of this enzyme. Here, we describe the links between the V_1 headpiece and the V_O-domain of the yeast V_1V_O ATPase via subunit A and *d* as well as the V_O subunits *a* and *d* using surface plasmon resonance and fluorescence correlation spectroscopy. Binding constants of about 60 and 200 nM have been determined for the *a*–*d* and *d*–A assembly, respectively. The data are discussed in light of subunit *a* and *d* forming a peripheral stalk, connecting the catalytic A_3B_3 hexamer with V_O.

Structured summary:
MINT-7012054: *d* (uniprotkb:P32366) *binds* (MI:0407) to A (uniprotkb:P17255) by *fluorescence correlation spectroscopy* (MI:0052)
MINT-7012041: *d* (uniprotkb:P32366) *binds* (MI:0407) to A (uniprotkb:P17255) by *surface plasmon resonance* (MI:0107)
MINT-7012028: *d* (uniprotkb:P32366) *binds* (MI:0407) to *a* (uniprotkb:P32563) by *surface plasmon resonance* (MI:0107)

1. Introduction

The vacuolar H^+-ATPase (V_1V_O ATPase) can be described as master element for energizing and maintaining homeostasis by directly controlling the vesicular transport at both exocytotic and endocytotic pathways of eukaryotic cells [1–5]. The V_1V_O ATPase is composed of a water-soluble V_1 ATPase and a membrane subcomplex, V_O [6]. The proton transducting V_O sector contains five different subunits in a stoichiometry of $a_1 : d_1 : c_{4-5} : c'_1 : c''_1$, whereby the V_1 sector is composed of eight subunits in a proposed stoichiometry of A_3:B_3:C_1:D_1:E_X:F_1:G2:H_x [7,8]. The energy, needed for proton translocation, is provided from the cleavage of adenosine triphosphate into adenosine diphosphate and inorganic phosphate, catalyzed in the A_3:B_3 hexamer of the V_1 headpiece. This energy-coupling between the A_3B_3 headpiece occurs via the '*stalk*' structure, an assembly of the V_1 and V_O subunits C, D, E, F, G, H and subunit *a* as well as *d*, respectively, forming the functional and structural interface [9]. The V_O complex can be subdivided into two parts, which are proposed to rotate relative to each other, the peripheral stalk and the proton-translocating ring. The V_O part of the peripheral stalk is proposed to consist of the N-terminal segment of subunit *a* and subunit *d* [7,9]. The proton-translocating ring comprises the subunits *c*, *c'* and *c''* [7,8]. The fifth V_O subunit, subunit *d*, has a boxing glove-shape in solution, made-up of a more globular domain and a protuberance [10] and is exposed on the cytoplasmic side of the membrane [10,11]. This protein plays a role in coupling ATP cleavage and proton transport [12] and is also essential for embryonic development [13]. In contrast, no structural details are known for subunit *a*, reported to be essential for proton translocation due to its C-terminal and membrane-embedded part (*a405-840*, [5]). The cytoplasmic and N-terminal segment of subunit *a* (*a1-388*, [5]) is proposed to bind to the protuberance of subunit *d* as shown by a structural comparison of the low-resolution structure of subunit *d* and the 3D-reconstruction of the V_O-sector (see Fig. 1A [10,11]). Previous work, using immunoprecipitation assays, has shown that the so-called non-homologous region (NHR) of the catalytic A subunit of the yeast V-ATPase co-precipitates with the V_O subunits *a* and *d* [14]. However, a complete understanding of these binding partners and their binding strength is lacking.

Abbreviations: DTT, dithiothreitol; FCS, fluorescence correlation spectroscopy; IPTG, isopropyl-β-D-thio-galactoside; NBD-Cl, 7-chloro-4-nitrobenzo-2-oxa-1,3-diazole; NHR, non-homologous region; NTA, nitrilotriacetic acid; PAGE, polyacrylamide gel electrophoresis; PCR, polymerase chain reaction; SAXS, small angle X-ray scattering; SDS, sodium dodecyl sulfate; SPR, surface plasmon resonance; TMR, tetramethylrhodamin; Tris, Tris-(hydroxymethyl) aminomethane

* Corresponding author. Fax: +65 6791 3856.
E-mail address: ggrueber@ntu.edu.sg (G. Grüber).

[1] Authors have equal contribution.

0014-5793/$36.00 © 2009 Federation of European Biochemical Societies. Published by Elsevier B.V. All rights reserved.
doi:10.1016/j.febslet.2009.03.013

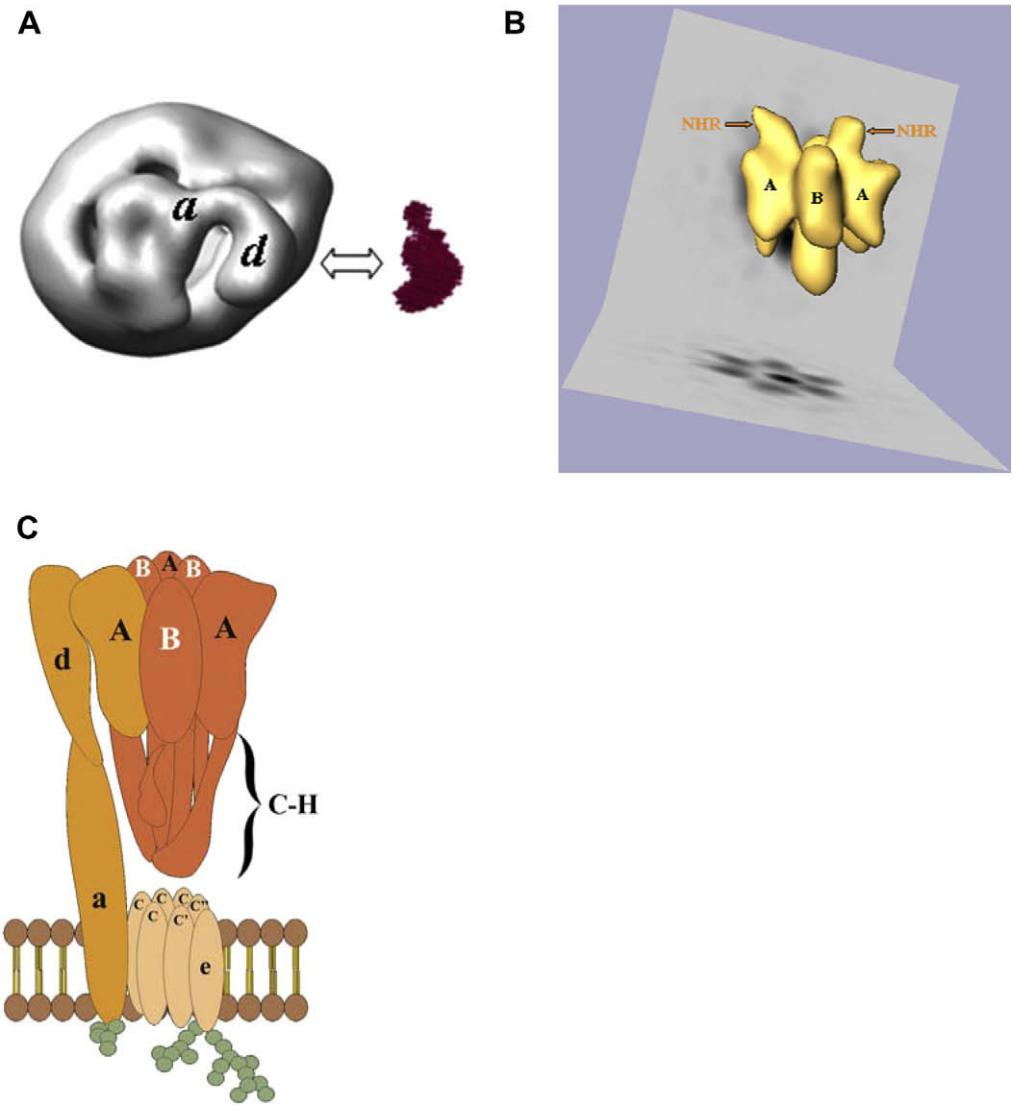

Fig. 1. (A) Shape comparison of the structure of subunit *d* (right) from yeast [10] with the predicted position of subunit *d* inside the three-dimensional reconstruction of the V_O domain from clathrin-coated vesicles (*left*) [11]. (B) Surface view of the 3D reconstruction of the V_1(-C) from *M. sexta* [16]. The alternating subunits A and B can be distinguished by the non-homologous regions of subunit A. (C) Topology of the V_1 (*orange*) and V_O section (*beige*) of the V-ATPase. In the V-ATPase the V_1 part can be reversibly disconnected from the V_O sector. The subunits *a*, *d* and A, studied in this work, are highlighted in ocher.

We have turned our attention to examine the interaction of subunit *a* and *d* of the V-ATPase from yeast to determine for the first time the binding affinity between both V_O subunits using surface plasmon resonance (SPR). The interaction among subunit *d* and the nucleotide-binding and NBD-Cl sensitive A subunit has been observed by fluorescence correlation spectroscopy (FCS) and SPR.

2. Materials and methods

2.1. Protein production and purification

Subunit *d* of the *Saccharomyces cerevisiae* V-ATPase was purified according to [10]. Cloning, production and purification of subunit A and $a_{1\text{-}388}$ are described under Supplementary data.

2.2. CD and FCS

Circular dicroism- and FCS spectra were measured using a CHIRASCAN spectropolarimeter and a LSM-FCS system, respectively, as described recently ([15] see Supplementary data).

2.3. SPR measurements

Surface plasmon resonance was performed using a Biacore 3000 instrument (see Supplementary data).

3. Results and discussion

3.1. Binding of subunit d with $a_{1\text{-}388}$

Recently, subunit *d* (Vma6p) of the yeast V_1V_O ATPase was generated, enabling to determine a low-resolution structure of the eukaryotic *d* [10]. Subunit *d* reveals a boxing glove-shaped molecule, consisting of two distinct domains (Fig. 1A [10]). This structure is similar to the elongated mass located above the V_O domain of the cytoplasmic site of the clathrin-coated vesicles [11]. Such topological arrangement indicates that *d* is connected via its protuberance to the N-terminus of subunit *a*, and supports the association of both proteins as predicted from mutagenesis studies in which cells lacking *a*, the subunit *d* is found in the cytosol [7]. To confirm the *a*–*d* association and to determine their binding constant, the N-terminal domain of subunit *a* (*Vph1p*) from

yeast, $a_{1\text{-}388}$ (*Vph1p*$_{1\text{-}388}$), has been produced and purified (Fig. 2A). The secondary structure of $a_{1\text{-}388}$ was obtained from CD spectra (Fig. 2B). The minima and the maximum indicate the presence of α-helices. The secondary structure content was 56% α-helix, 12% β-sheet and 32% random coil, consistent with secondary structure predictions. Subunit *d* [10] and $a_{1\text{-}388}$ were used for kinetic analysis of the interaction using surface plasmon resonance. Immobilized subunit *d* was used to study binding affinity kinetics with subunit *a*. An association rate constant $k_a = 7.7\ (\pm 1.1) \times 10^3\ M^{-1}\ s^{-1}$ and dissociation rate constant $k_d = 4.4\ (\pm 1.2) \times 10^{-4}\ s^{-1}$ was obtained (Fig. 3). Consequently a dissociation constant (k_d/k_a) of $K_D = 6.0\ (\pm 1.8) \times 10^{-8}$ M was determined for binding between the V_O subunits $a_{1\text{-}388}$ and *d*.

3.2. Subunit d and A assembly

Immunoprecipitation of the non-homologous regions (NHR) of subunit A from cells producing only the NHR segment showed co-precipitation with the V_O subunits *a* and *d* [14]. Fig. 1B reveals that the NHR domain is at the top of subunit A and thereby in the upper part of the A_3B_3 hexamer [16]. Since subunit *d* is forming the tip of the cytoplasmatic mass of V_O sector, which might go up during V_1V_O assembly, we intended to study the closeness of subunit *d* and A. Subunit A was produced in high purity (Fig. 5A). Its ATP binding capacity was proven by FCS. Fig. 4A shows the autocorrelation curves of the ATP-analog, MgATP ATT0-647N in the absence and presence of A. The addition of protein resulted in a change of the mean diffusion time τ_D. The increase of the diffusion time was due to the increase in the mass of the diffusing particle, when the nucleotide bound to the protein. A binding constant (*K*) of 110 ± 1.9 μM of bound MgATP ATT0-647N to subunit A was calculated (Fig. 4B).

7-Chloro-4-nitrobenzo-2-oxa-1,3-diazole (NBD-Cl) has been found to inhibit the V_1V_O ATPase [17] and the F_1F_O ATP synthase [18,19]. In F_1F_O ATP synthase, NBD-Cl reacts with a Tyr residue in the central nucleotide-binding domain of the catalytic subunit β,

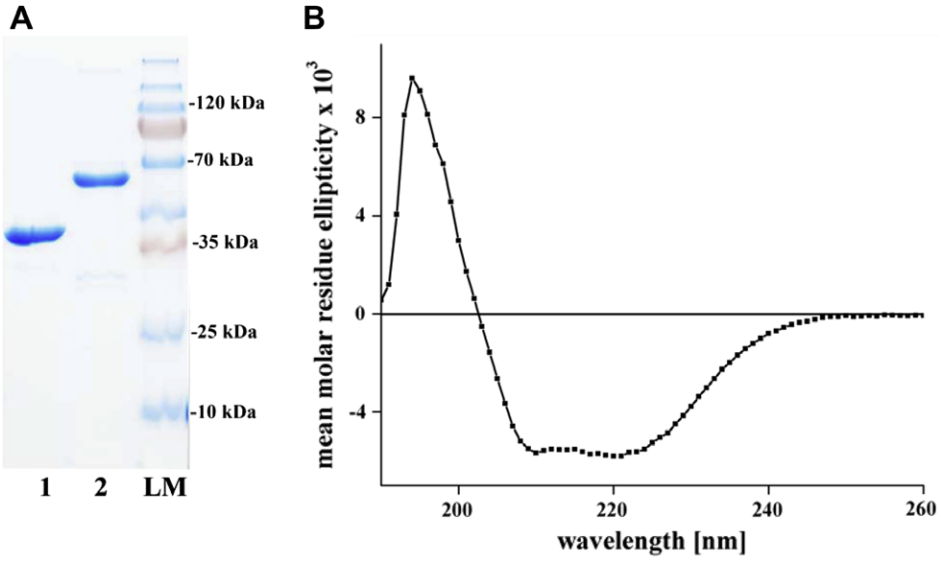

Fig. 2. (A) SDS–PAGE of $a_{1\text{-}388}$ (*lane 1*), subunit A (*lane 2*) and protein marker (*lane 3*). (B) UV-CD spectrum of $a_{1\text{-}388}$ of the yeast V-ATPase.

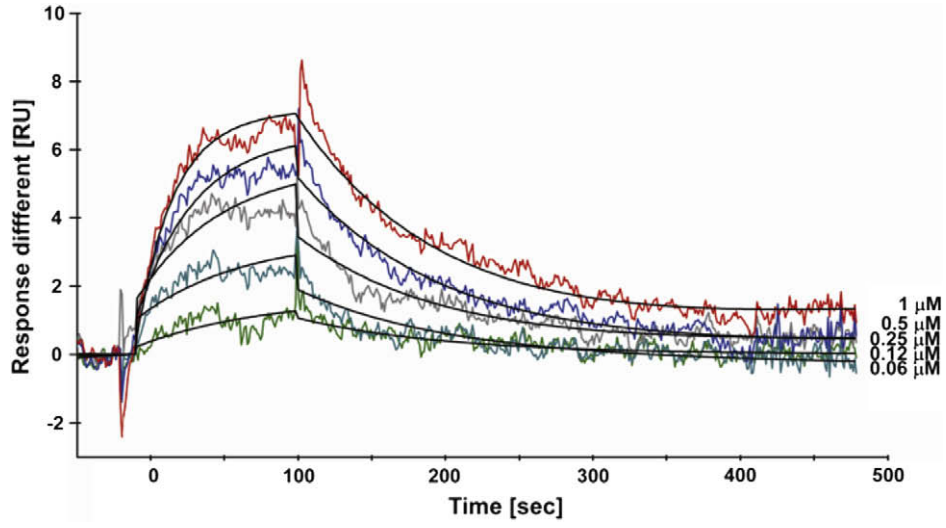

Fig. 3. Binding responses and kinetic analysis using SPR for the *a*–*d* interaction. The experiment was performed by passing subunit *a* at different concentrations (62.5, 125, 250, 500, 1000 nM) over the immobilized subunit *d* surface.

which is the homolog to subunit A, resulting in the loss of the lowest affinity binding site for nucleotides [18]. By comparing the autocorrelation curves of the subunit A-ATP-ATT0-647N bound form with those, in which the protein has been preincubated with increasing amounts of NBD-Cl, the diffusion time of ATP ATT0-647N was shown to decrease with increasing concentrations of NBD-Cl (Fig. 4C), indicating that nucleotide-binding to subunit A became inhibited. A concentration of about 270 μM of NBD-Cl dropped the ATP-binding capacity to 50% (Fig. 4D). These data indicate that the protein used in these studies is functional active.

Firstly, binding of subunit A to *d* was analyzed by FCS, whereby subunit *d* (Fig. 5A) was labeled with TMR. Fig. 5B shows the autocorrelation curves for the labeled *d* in the absence and presence of subunit A. The addition of subunit A caused a change in the mean diffusion time τ_d, which increased with rising concentrations. The increase in the diffusion time was due to the increase in the mass of the diffusing particle when subunit *d*-TMR interacted with subunit A. A binding constant of 200 ± 15 nM for binding of subunit *d*-TMR to subunit A was calculated (Fig. 5C). By contrast, when TMR-labeled subunit *a* has been titrated with A no significant binding could be observed (data not shown). The strong binding of subunits *a* and *d* and the specificity of the *d*–A assembly indicate that the proteins used in these studies are reconstitutively active.

To confirm the A–*d* assembly SPR experiments have been done, in which subunit *d* was immobilized. The $k_a = 2.4 \times 10^4$ (±0.5) $M^{-1}\,s^{-1}$ and $k_d = 6.4 \times 10^{-3}$ (±0.4) s^{-1} were obtained, resulting in a K_D value of 2.7×10^{-7} M (±0.5) (Fig. 5D). The sensorgrams appear to have a slight biphasic behavior, which could derive from heterogeneity of the surface due to the amine coupling of subunit *d* to the sensor surface, or from a difference in refractive index of sample and running buffer. The Biaevaluation software had taken into account a refractive index difference between the sample and the running buffer, which made the sensorgrams appear biphasic. The affinity value for the interaction is very similar to the value obtained from FCS. The data were also analyzed using the Scrubber 2 software, confirming the monophasic binding profile (Supplementary Fig. S1). The FCS and SPR data presented here clearly demonstrate that subunit A does bind to *d*, indicating that *d* is accessible in the complex. This confirms the results from mild proteolysis experiments of the V_1V_O ATPase in intact clathrin-coated vesicles, in which rapid cleavage of *d* was observed, suggesting that it is exposed inside the enzyme [20,21]. This is also in line with the observation, that the N-terminal segment of *a*

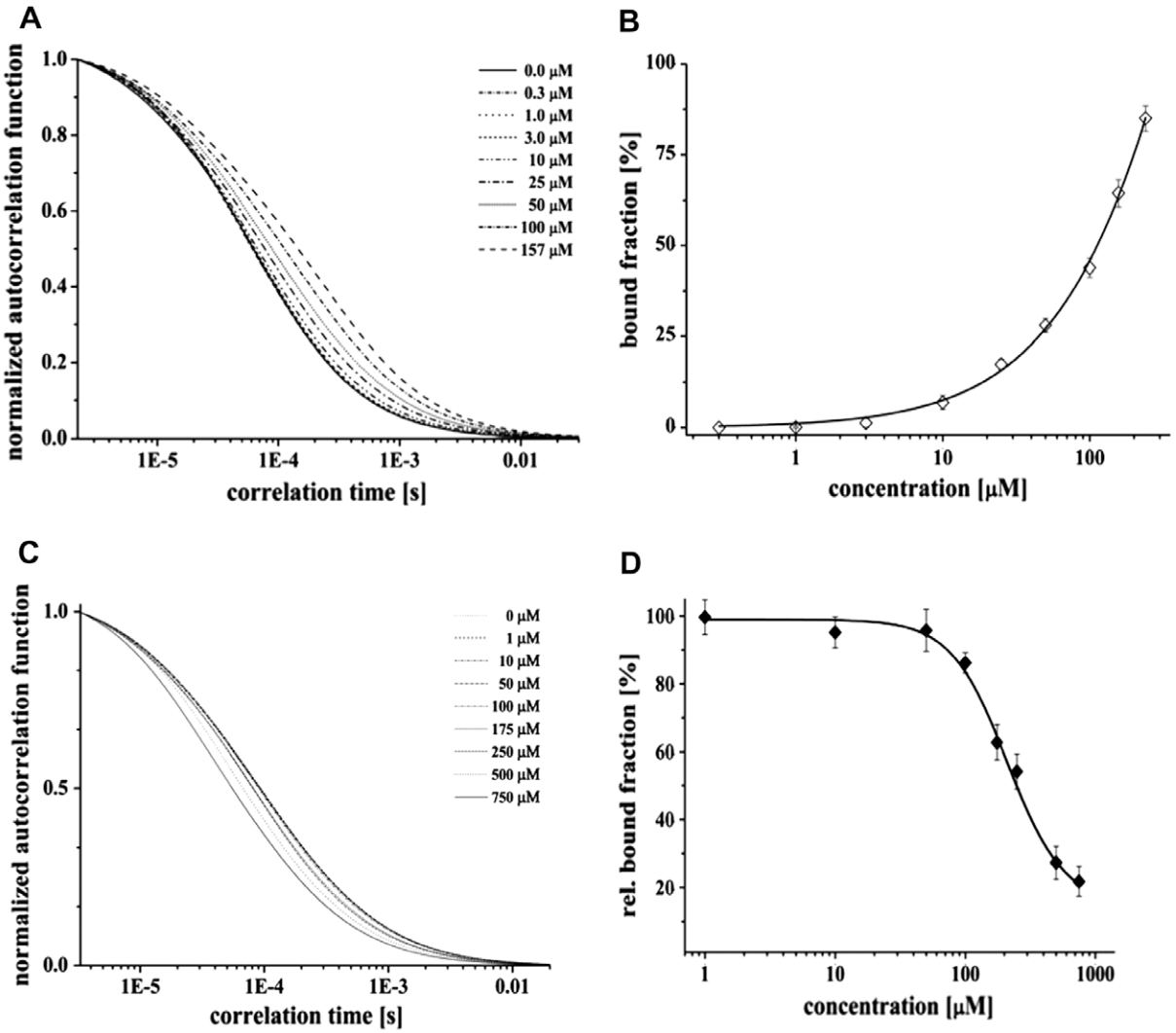

Fig. 4. (A) Normalized autocorrelation functions of MgATP ATTO-647N by increasing the amount of subunit A. (B) Concentration-dependent binding of subunit A MgATP-ATT0-647N. (C) Normalized autocorrelation functions of labeled ATP obtained by increasing the amount of NBD-Cl (from left to right: 0 to 750 μM). (D) Concentration-dependent influence of NDB-Cl versus Mg-ATP binding to subunit A.

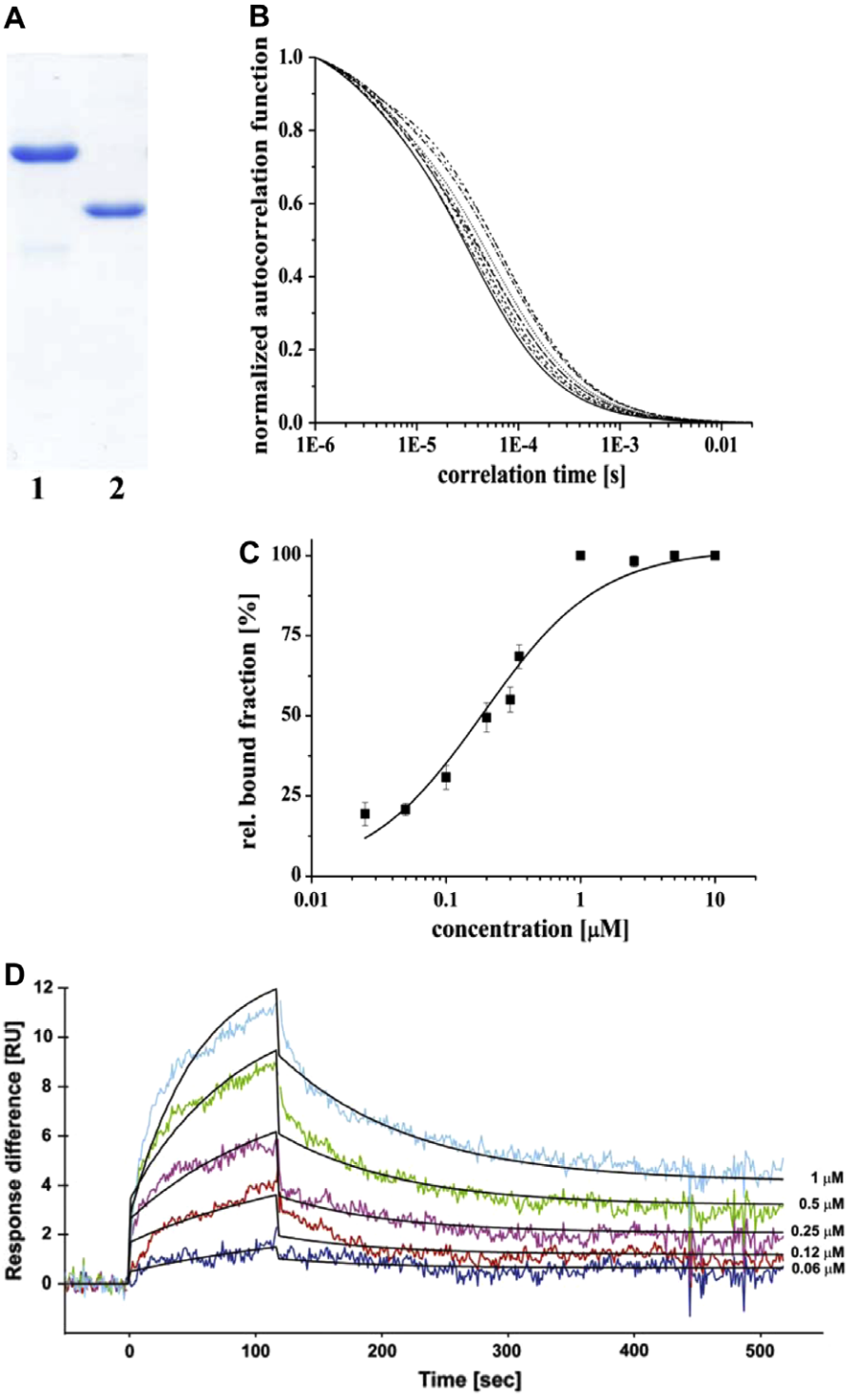

Fig. 5. Subunit A binding to subunit *d* studied by FCS (B and C) and SPR (D). (A) SDS–PAGE revealing subunit A (*lane 1*) and *d* (*lane 2*). (B) Normalized autocorrelation functions of subunit *d* labeled by TMR obtained by increasing the quantity of A. (B) Concentration-dependent binding of subunit A versus *d*. (C) Binding responses and kinetic analysis of the *d*–A interaction. Subunit A was used in the concentration range of 0.06–1 μM.

becomes accessible for degradation only in the absence of *d* [22]. Models were described in which subunit *a* and *d* do form a peripheral stalk, thereby linking the V_O sector with the A_3B_3 headpiece [10,23]. Like in the case of the peripheral stalk subunit *b* of the F_1F_O ATP synthase, laterally located cytoplasmic part of subunit *b* seen in F_O [24] moves up after assembly with the F_1 sector, connecting F_O with the N-terminal part of the $\alpha_3\beta_3$-headpiece of F_1 [25]. Taking this into account the cavity of the boxing glove-shaped *d* may enable the *a*–*d* domain to bind to the NHR of A in the process of reversible V_1 and V_O association (Fig. 1C). The NHR is linked to both coupling of proton transport and ATP hydrolysis and dissociation of the V_1V_O ATPase *in vivo* [14]. Dissociation and reassociation of V_1 and V_O in the yeast V-ATPase is glucose dependent [26]. As shown by immunoprecipitation assays removal of glucose disrupts the assembly of the NHR from the V_O domain, whereby addition of glucose causes the reassociation of an NHR, subunit *a* and *d* assembly [14], reflecting the relevance of knowing the partners forming this peripheral stalk. The extended assembly of *a* and

d provides the surface for the interaction of *a* with the GDP/GTP exchange factor ARNO (ADP-ribosylation factor nucleotide site opener) [27], and at the same time making V_O accessible for its association with GTPase Arf6. Such an interaction of the V-ATPase with ARN) and Arf6 has recently been found in early endosomes [1,28].

Acknowledgment

This research was supported by the School of Biological Sciences, NTU. Y.R. Thaker is grateful to the Nanyang Technological University for awarding research scholarship.

Appendix A. Supplementary data

Supplementary data associated with this article can be found, in the online version, at doi:10.1016/j.febslet.2009.03.013.

References

[1] Marshansky, V. (2007) The V-ATPase a2-subunit as a putative endosomal pH-sensor. Biochem. Soc. Trans. 35, 1092–1099.
[2] Saroussi, S. and Nelson, N. (2009) Vacuolar H^+-ATPase-an enzyme for all seasons. Pflugers Arch. – Eur. J. Physiol. 457, 581–587.
[3] Beyenbach, K.W. and Wieczorek, H. (2006) The V-type H^+ ATPase: molecular structure and function, physiological roles and regulation. J. Exp. Biol. 209, 577–589.
[4] Kluge, C., Lahr, J., Hanitzsch, M., Bolte, S., Golldack, D. and Dietz, K.-J. (2003) New insight into the structure and regulation of the plant vaculoar H^+-ATPase. J. Bioenerg Biomembr. 35, 377–388.
[5] Marshansky, V. and Futai, M. (2008) The V-type H^+-ATPase in vesicular trafficking: targeting, regulation and function. Curr. Opin. Cell Biol. 20, 415–426.
[6] Lolkema, J.S., Chaban, Y. and Boekema, E.J. (2003) Subunit composition, structure, and distribution of bacterial V-type ATPase. J. Bioenerg Biomembr. 35, 323–336.
[7] Graham, L.A., Flannery, A.R. and Stevens, T.H. (2003) Structure and assembly of the yeast V-ATPase. J. Bioenerg Biomembr. 35, 301–312.
[8] Inoue, T., Wilkens, S. and Forgac, M. (2003) Subunit structure, function and arrangement in the yeast and coated vesicle V-ATPase. J. Bioenerg Biomembr. 35, 291–299.
[9] Müller, V. and Grüber, G. (2003) ATP syntases: structure, function and evolution of unique energy converters. Cell Mol. Life Sci. 60, 474–494.
[10] Thaker, Y.R., Roessle, M. and Grüber, G. (2007) The boxing glove shape of subunit d of the yeast V-ATPase in solution and the importance of disulfide formation for folding of this protein. J. Bioenerg Biomembr. 39, 275–289.
[11] Wilkens, S. and Forgac, M. (2001) Three-dimensional structure of the vacuolar ATPase proton channel by electron microscopy. J. Biol. Chem. 276, 44064–44068.
[12] Nishi, T., Kawasaki-Nishi, S. and Forgac, M. (2003) Expression and function of the mouse V-ATPase d subunit isoforms. J. Biol. Chem. 278, 46396–46402.
[13] Miura, G.I., Froelick, G.J., March, D.J., Stark, K.L. and Palmiter, R.D. (2003) The d subunit of the vacuolar ATPase (ATP6d) is essential for embryonic development. Transgenic Res. 12, 131–133.
[14] Shao, E., Nishi, T., Kawasaki-Nishi, S. and Forgac, M. (2003) Mutational analysis of the non-homologous region of subunit A of yeast V-ATPase. J. Biol. Chem. 278, 12985–12991.
[15] Hunke, C., Chen, W.J., Schäfer, H.J. and Grüber, G. (2007) Cloning, purification, and nucleotide-binding traits of the catalytic subunit A of the V_1V_O ATPase from *Aedes albopictus*. Protein Expr. Purif. 53, 378–383.
[16] Radermacher, M., Ruiz, T., Wieczorek, H. and Grüber, G. (2001) Three-dimensional electron microscopy reveals the structure of the V_1-ATPase. J. Struct. Biol. 135, 26–37.
[17] Schirmanns, K. and Zeiske, W. (1994) An investigation of the midgut K^+-pump of the tobacco hornworm (*Manduca sexta*) using specific inhibitors and amphotericin B. J. Exp. Biol. 188, 191–204.
[18] Orriss, G.L., Leslie, A.G., Braig, K. and Walker, J.E. (1998) Bovine F_r ATPase covalently inhibited with 4-chloro-7-nitrobenzofurazan: the structure provides further support for a rotary catalytic mechanism. Structure 6, 831–837.
[19] Weber, J., Wilke-Mounts, S. and Senior, A.E. (1994) Cooperativity and stoichiometry of substrate binding to the catalytic sites of *Escherichia coli* F_1-ATPase. Effects of magnesium, inhibitors, and mutation. J. Biol. Chem. 269, 20462–20467.
[20] Bauerle, C., Ho, M.N., Lindorfer, M.A. and Stevens, T.H. (1993) The *Saccharomyces cerevisiae* vma6 gene encodes the 36-kDa subunit of the vacuolar H^+-ATPase membrane sector. J. Biol. Chem. 268, 12749–12757.
[21] Wang, S.Y., Moriyama, Y., Mandel, M., Hulmes, J.D., Pan, Y.C., Danho, W., Nelson, H. and Nelson, N. (1988) Cloning of cDNA encoding a 32 kDa protein: an accessory polypeptide of the H^+-ATPase from chromaffin granules. J. Biol. Chem. 263, 17638–17642.
[22] Adachi, I., Puopolo, K., Marquez-Sterling, N., Arai, H. and Forgac, M. (1999) Dissociation, cross-linking, and glycosylation of the coated vesicle proton pump. J. Biol. Chem. 265, 967–973.
[23] Forgac, M. (1999) Structure and properties of the vacuolar (H^+)-ATPase. J. Biol. Chem. 274, 12951–12954.
[24] Singh, S., Turina, P., Bustamante, C.J., Keller, D.J. and Capaldi, R.A. (1996) Topographical structure of membrane-bound *Escherichia coli* F_1F_O ATP synthase in aqueous buffer. FEBS Lett. 397, 30–34.
[25] Wilkens, S. and Capaldi, R.A. (1998) Electron microscopic evidence of two stalks linking the F_1 and F_O parts of the *Escherichia coli* ATP synthase. Biochim. Biophys. Acta 1365, 93–97.
[26] Kane, P.M. (1995) Disassembly and reassembly of the yeast vacuolar H^+-ATPase in vivo. J. Biol. Chem. 270, 17025–17032.
[27] Frank, S., Upender, S., Hansen, S.H. and Casanova, J.E. (1998) ARNO is a guanine nucleotide exchange factor for ADP-ribosylation factor 6. J. Biol. Chem. 273, 23–27.
[28] Hurtado-Lorenzo, A., Skinner, M., Annan, J.E., Futai, M., Sun-Wada, G.-H., Bourgoin, S., Casanova, J., Wildeman, A., Bechoua, S., Ausiello, D.A., Brown, D. and Marshansky, V. (2006) V-ATPase interacts with ARNO and Arf6 in early endosomes and regulates the protein degradative pathway. Nat. Cell Biol. 8, 124–136.